



Discrimination between breast invasive ductal carcinomas and benign lesions by optimizing quantitative parameters derived from dynamic contrast-enhanced MRI using a semi-automatic method

Jiawen Yang¹ · Jiandong Yin²

Received: 26 December 2018 / Accepted: 21 February 2019 / Published online: 27 February 2019
© Japan Society of Clinical Oncology 2019

Abstract

Background To propose a semi-automatic method for distinguishing invasive ductal carcinomas from benign lesions on breast dynamic contrast-enhanced magnetic resonance imaging (DCE-MRI).

Methods 142 cases were included. In the conventional method, the region of interest for a breast lesion was drawn manually and the corresponding mean time–signal intensity curve (TIC) was qualitatively categorized. Only one quantitative parameter was obtained: the maximum slope of increase (MSI). By contrast, the proposed method extracted the suspicious breast lesion semi-automatically. Besides MSI, more quantitative parameters reflecting perfusion information were derived from the mean TIC and lesion region, including the signal intensity slope (SI_{slope}), initial percentage of enhancement, percentage of peak enhancement, early signal enhancement ratio, and second enhancement percentage. The mean TIC was categorized quantitatively according to the value of SI_{slope} . Regression models were established. The diagnostic performance differed between the new and conventional methods according to the Wilcoxon rank-sum test and receiver operating characteristic analysis.

Results According to the TIC categorization results, the accuracies of the traditional and the new method were 59.16% and 76.05%, respectively ($P < 0.05$). The accuracy was 63.35% for MSI, which was derived from the manual method. For the semi-automatic method, the accuracies were 81.0% and 78.9% for the lesion region and the corresponding mean TIC regression models, respectively.

Conclusions The results demonstrate that our proposed semi-automatic method is beneficial for discriminating breast IDCs and benign lesions based on DCE-MRI, and this method should be considered as a supplementary tool for subjective diagnosis by clinical radiologists.

Keywords Invasive ductal carcinoma · MRI · Receiver operating characteristic · Regression analysis

Introduction

Breast cancer is the most common malignant tumor in women and it is now the most frequently diagnosed cancer. Throughout the world, breast cancer is the leading cause (14%) of cancer-related deaths in females [1]. Invasive ductal carcinoma (IDC) is the most common type of breast cancer [2]. Image detection plays an important

role in the early diagnosis, treatment, and prognosis for breast cancer, and several modalities are employed for breast imaging, for example mammography, ultrasound, dynamic contrast-enhanced magnetic resonance imaging (DCE-MRI), and breast computed tomography (CT) [3–6]. Mammography is the main imaging screening method for breast cancer, but it is affected significantly by breast density. Ultrasound is not sensitive to microcalcifications, and breast CT requires a large dose of radiation. DCE-MRI is potentially valuable for breast cancer screening compared with these other examination methods [3–5]. The use of DCE-MRI for screening and diagnosing breast cancer has increased in recent years [7, 8]. In general, a manual method is used for the analysis of breast DCE-MRI results, but this approach is usually affected by inter-observer variability and partial volume

✉ Jiandong Yin
jiandongyin@sina.com

¹ Department of Equipment, Shengjing Hospital of China Medical University, Shenyang, China

² Department of Radiology, Shengjing Hospital of China Medical University, Shenyang, China

effects. Moreover, the manual method is time consuming. Time–signal intensity curves (TICs) of breast lesions are used widely in dynamic analysis, where quantitative parameters that reflect perfusion information are calculated based on the TICs, including the maximum slope of increase (MSI), signal intensity slope (SI_{slope}), initial percentage of enhancement (E_{initial}), percentage of peak enhancement (E_{peak}), early signal enhancement ratio (ESER), and second enhancement percentage (SEP) [9–13]. However, these parameters have been investigated separately to assess the diagnostic performance, so it is still unclear which parameters are most useful for diagnosis, or whether several parameters can be combined to further improve the diagnostic performance.

Hence, in this study, we developed a novel method for semi-automatically analyzing breast DCE-MRI data, where the lesions were extracted semi-automatically and more quantitative parameters were measured. Unlike previous studies, we applied regression analysis to the separate parameters, and a diagnostic model was established by weighting these parameters after selection using independent sample t tests. To the best of our knowledge, no previous studies have employed this approach, and we hope that our results can further improve the diagnostic performance of breast DCE-MRI.

Materials and methods

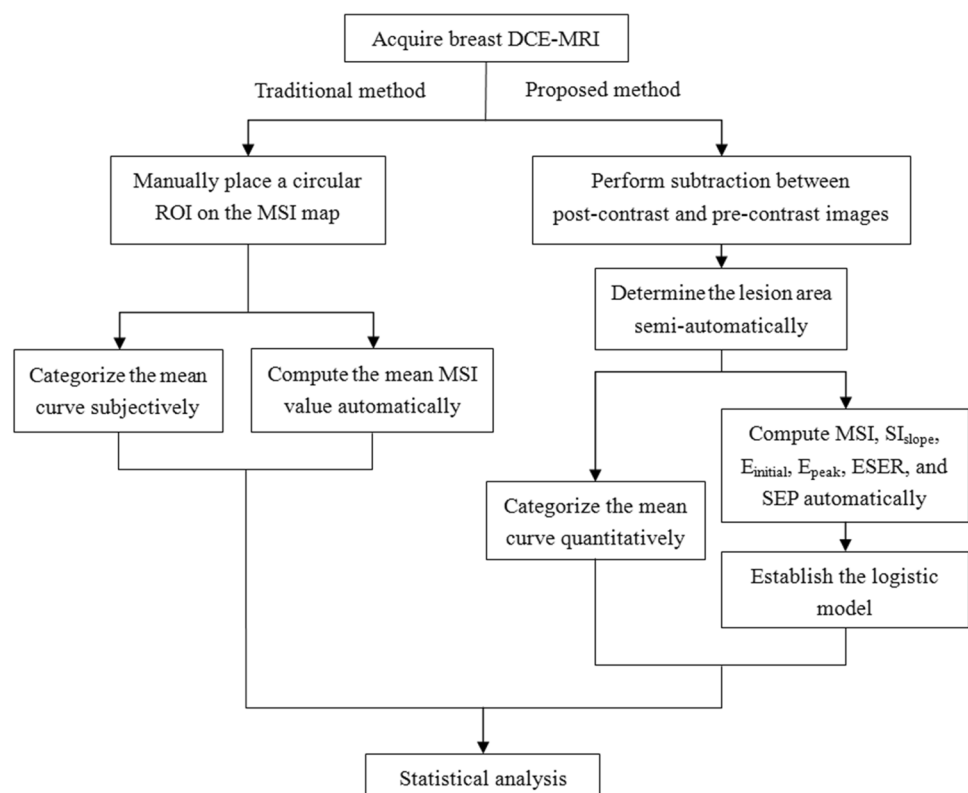
Figure 1 shows the experimental procedure in this study. The traditional method utilized FuncTool 9.4.05A (GE Healthcare, Milwaukee, WI, USA) on the work station to analyze the TICs. By contrast, the proposed semi-automatic method extracted the lesion regions and obtained all of the quantitative parameters with MATLAB (version R2010b, The MathWorks, Inc., Natick, MA, USA).

Patients

This study was approved by the ethics committee of Shengjing Hospital (No. 2013PS113K). The method used in this study was performed in accordance with the approved guidelines. All of the images used in this study were collected from our existing picture archiving and communication system (PACS) database. The requirement for informed content was waived because this was a retrospective study. The breast DCE-MRI images collected between January 2009 and August 2014 were analyzed retrospectively by a radiologist. All the images were anonymised.

All of the patients received breast MRI examinations for the first time and all of the cases that we retrospectively selected from our PACS contained lesions. MRI examinations were used to determine the properties of lesions rather

Fig. 1 Flowchart illustrating the process followed in this study



than staging or family history, especially to distinguish malignant and benign lesions. Although they received the mammography examinations, some uncertain diagnostic cases were referred for MRI examinations because of the limitations of this imaging modality. The clinicians of some other patients asked directly for MRI examinations.

The patient selection criteria for our study were summarized in Fig. 2. All of the selected lesions were single lesions presenting a mass-like shape, occurring in either the left or right breast. In addition, each lesion was confirmed as benign or malignant by biopsy or pathology (the time interval between MRI and histopathological examination was < 5 days). Following the above inclusion criteria, 1465 cases were excluded from the subsequent analysis. Because the majority of malignant tumors comprised IDCs, only IDCs were selected for subsequent analysis.

DCE-MRI examination

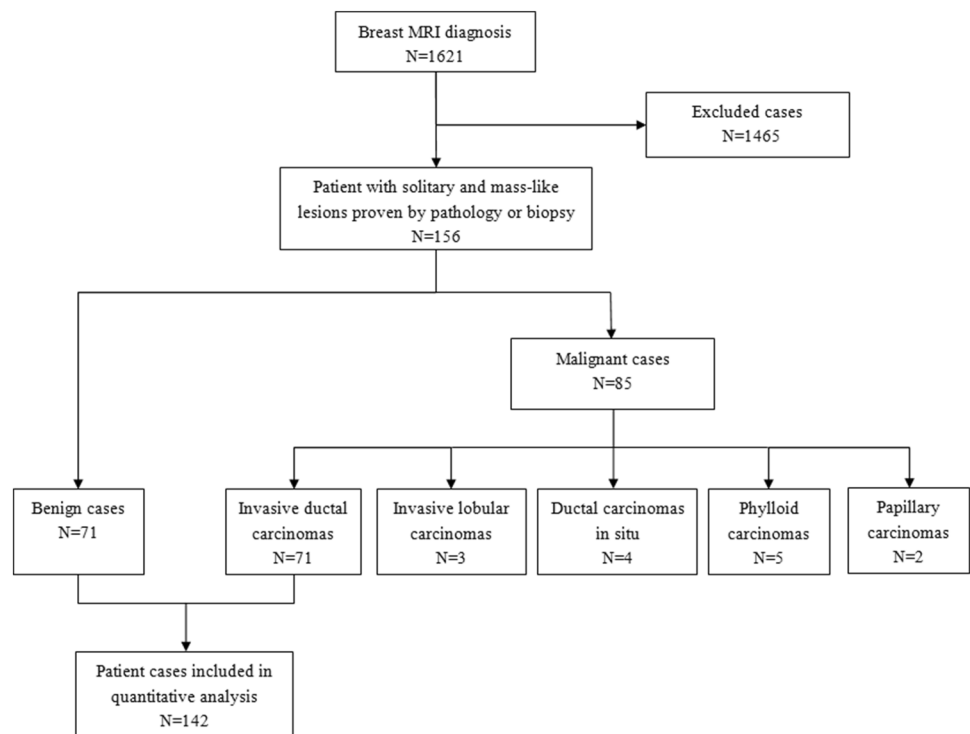
All of the MRI examinations were performed using a 3.0T system (Signa HDxt, GE Healthcare, Milwaukee, WI, USA) with a dedicated eight-channel breast coil. Patients were in the prone position. The breast DCE-MR images were obtained using the VIBRANT-VX technique with the following parameters: repetition time = 7.42 ms, echo time = 4.25 ms, inversion time = 20 ms, echo train length = 1, slice thickness = 2.2 mm, spacing between slices = 2.2 mm, flip angle = 15°, image size = 1024 × 1024, pixel spacing = 0.3516 mm, acquisition type = 3D, and slice

number = 78. The contrast agent (0.5 mmol/ml gadodiamide; Omniscan, GE Healthcare, Magnevist, Bayer-Schering Pharmaceuticals) was delivered intravenously by a power injector with a dosage of 0.15 mmol/kg bodyweight at a rate of 4 ml/s, followed by an equal volume of saline flush at the same flow speed. The temporal acquisition was 80 s for each volume image, and the dynamic series comprised nine individual dynamic images, i.e., one obtained before and eight after injecting the contrast agent. Hence, the total dynamic scanning time was 720 s (80 × 9). The subtracted MR images (the post-contrast images minus the pre-contrast images) were acquired for extracting lesion regions. The subtracted volume image was analyzed and the slice image with the lesion of maximum size was selected for subsequent analysis.

Traditional method

A highly experienced radiologist (13 years work experience in breast MRI) who was blinded to the clinical history and pathology results manually analyzed the TICs using the commercially available software tool installed on the MRI work station. First, a circular region of interest (ROI) was placed on the color-coded MSI map to draw the lesion manually. In routine practice, the ROI was smaller than the lesion area. Next, the corresponding mean TIC was plotted automatically for the ROI. The radiologist discriminated between the benign and malignant cases according to the shape of the

Fig. 2 The patient flow



mean TIC. Finally, the unique quantitative parameter, MSI, was obtained using the following formula:

$$MSI = \max(SI_{i+1} - SI_i), \quad (1)$$

where SI_i indicates the signal intensity at any time point (i ranges from 0 to 7).

Semi-automatic method

All the digital imaging and communication of medicine (DICOM) images were directly processed using MATLAB. The proposed method was performed according to the following steps.

First, subtraction was performed between the post-contrast and pre-contrast images.

Second, a ROI was drawn around the lesion, and then a popular segmentation method, OTSU, was applied to distinguish background and foreground pixels with the optimal threshold obtained by maximizing the variance [14]. Meanwhile, the segmented image was converted into a binary image.

Third, morphological erosion with a template of 3×3 matrix was applied to the binary image, and the unique but largest eight-connected region was selected. Then, morphological dilation with the above mentioned template was applied to the unique region and the target lesion region was obtained.

Fourth, the mean TIC of the lesion region was plotted automatically.

Finally, all of the quantitative parameters (E_{initial} , E_{peak} , ESER, SEP, MSI, and SI_{slope}) were calculated automatically using the following formulae [9–13]:

1. SI_{slope}

$$SI_{\text{slope}} = [(SI_{\text{tail}} - SI_{\text{mean}})/SI_{\text{mean}}] \times 100\%. \quad (2)$$

SI_{mean} is the signal intensity at the 120 s [12]. In this study, it was replaced by the mean value of the first two post-contrast time points. SI_{tail} is the signal intensity at the last time point. According to the value of SI_{slope} , the TIC pattern can be categorized into three types: type I (persistent) when

the SI_{slope} is +10% or greater, type II (plateau) when the SI_{slope} is between -10% and +10%, and type III (washout) when the SI_{slope} is -10% or less [15, 16].

2. E_{initial}

$$E_{\text{initial}} = [(SI_1 - SI_0)/SI_0] \times 100\%. \quad (3)$$

SI_0 indicates the signal intensity before the contrast agent injection and SI_1 indicates the signal intensity at the first time point after injecting the contrast agent.

3. E_{peak}

$$E_{\text{peak}} = [(SI_{\text{peak}} - SI_0)/SI_0] \times 100\%. \quad (4)$$

SI_{peak} indicates the peak value of the contrast enhancement.

4. ESER

$$ESER = [(SI_1 - SI_0)/(SI_2 - SI_0)] \times 100\%. \quad (5)$$

SI_2 indicates the signal intensity at the second time point after injecting the contrast agent.

5. SEP

$$SEP = [(SI_2 - SI_0)/SI_0] \times 100\%. \quad (6)$$

All of these parameters were calculated using two methods. First, the mean TIC for the extracted lesion region was obtained and the above parameters were derived from the mean TIC. Second, the quantitative parameters for each TIC corresponding to every pixel in the extracted lesion region were calculated and averaged. The corresponding parametric maps were color-coded.

Statistical analysis

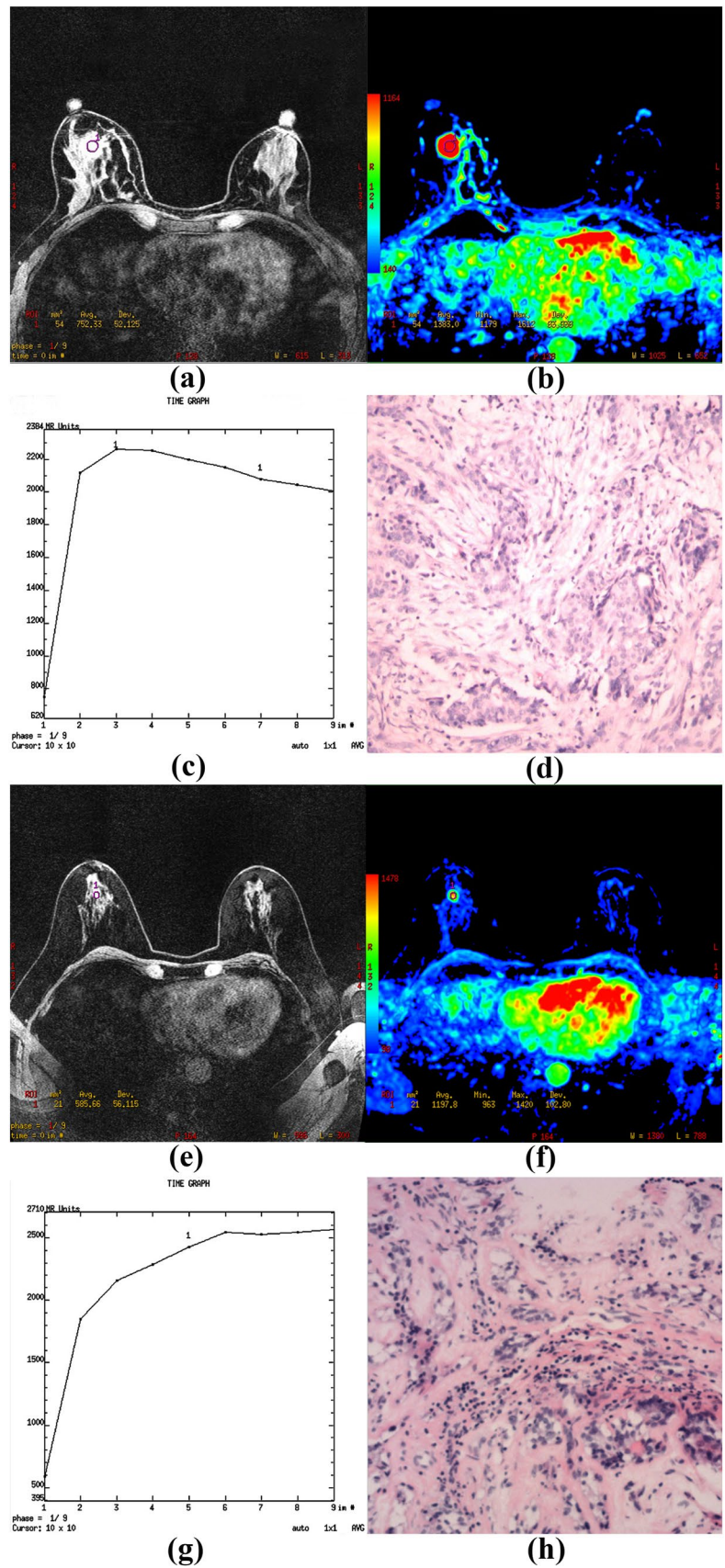
In this study, we established regression models for the quantitative parameters obtained with the two methods described previously. The logistic regression model was used to predict

Table 1 Detailed histopathological diagnoses for the benign breast lesions ($n = 71$)

Lesion type	<i>n</i>	%
High risk (complex sclerosing lesion, FEA, CCC with focal atypia)	5	7.04
Fibroadenoma, fibroadenomatous hyperplasia	33	46.48
Papilloma	4	5.63
DH, CCC, FCC, focal fibrosis, nodular sclerosing adenosis	16	22.54
Miscellaneous (chronic abscess, gynecomastia, fat necrosis, pseudoangiomatosis)	13	18.31

FEA flat epithelial atypia, CCC columnar cell changes, DH ductal hyperplasia, FCC fibrocystic changes

Fig. 3 Results obtained with manual method for one benign case and one malignant case, which were both selected randomly. The first two rows showed the results for the malignant case, IDC. **a** Pre-contrast image with the ROI drawn manually. **b** MSI color-coded map with ROI. **c** Mean curve of TICs obtained from the ROI. **d** Pathology result. **e-h** The last two rows showed the same results as a-d, only for the benign case



a binary response variable and to analyze the possible effects of the parameters. Principal component logistic regression was applied to obtain accurate estimates of the parameters in the models and to avoid co-linearity. First, the parameters were standardized and principal component logistic regression was then performed with SPSS (version 16.0) to establish the regression models with standardized parameters. The regression models were determined by a tenfold cross-validation strategy. *U* tests were performed to estimate the standardized parameters in the regression models. Finally, the standardized parameters were reverted to the original parameters.

The diagnostic performance of different methods was analyzed based on the receiver operating characteristic (ROC) using MedCalc (version 15.8). ROC curves were drawn for the regression model derived from the mean curve and for the regression model derived from the lesion region, respectively. In addition, the ROC curve was drawn for the MSI obtained by the manual method. The AUC and the optimal cutoff value were provided by MedCalc automatically. The corresponding sensitivity, specificity, and accuracy were also calculated. A higher AUC value indicated better diagnostic performance. For the TIC categorization, a Wilcoxon rank-sum test was performed to compare diagnostic accuracy between the manual method and the proposed method. The difference was considered significant with a *P* value less than 0.05.

Results

As a result, 142 cases (all female; age range 22–79 years; mean age 53.5 years) were collected (71 IDCs and 71 benign cases), and the details for benign cases are summarized in Table 1. The malignant lesion distribution was 34 left side and 37 right side lesions. The benign cases consisted of 29 left side and 42 right side lesions. The maximum size, averaged by independent measurements of two high-experienced radiologists, ranged from 6.7 to 44.3 mm.

Two cases were selected randomly to illustrate the results obtained by the manual method (Fig. 3). The results were produced using a commercial work station. Figure 4 shows the results obtained by the proposed method to differentiate between malignant and benign lesions in breast DCE-MR images, including the semi-automatically extracted lesions and color-coded maps for the quantitative parameters that reflect perfusion information.

Table 2 shows the principal component logistic regression models and the ROC analysis results. The other three parameters (E_{initial} , SEP, and E_{peak}) did not differ significantly between the benign lesions and IDCs (independent samples *t* test, $P > 0.05$). The estimates of the standardized

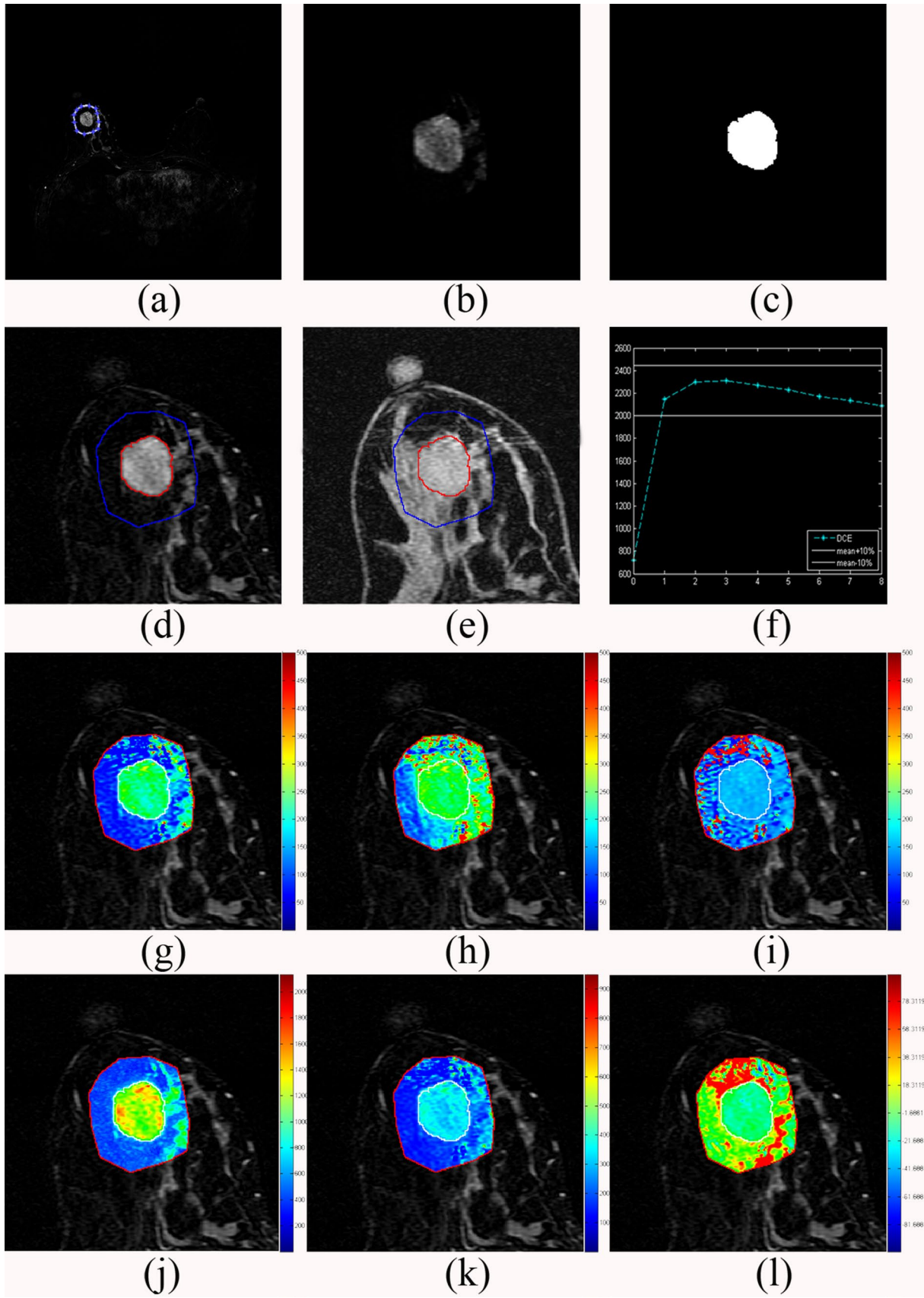
Fig. 4 Results obtained using the semi-automatic method. **a–f** Subtracted image, partially enlarged image, the determined lesion region, subtraction image with the lesion region (the ROI is delineated in blue and the lesion region in red), pre-contrast image with the lesion region, and mean TIC for the lesion region. **g–l** Color-coded MSI map, E_{initial} map, E_{peak} map, ESER map, SEP map, and SI_{slope} map

parameters (SI_{slope} , ESER, and MSI) in the regression models were significant ($U > 2.58$, $P < 0.01$). The AUC values representing the diagnostic performance are also shown in this table, as well as the optimal cutoff values, sensitivity, specificity, and accuracy. The AUC was higher for the regression model based on the lesion region compared with that based on mean curve. The ROC analysis results showed that the regression models based on the proposed method had higher clinical diagnostic performance than that based on the manually obtained MSI. The ROC curves are presented in Fig. 5.

The sensitivity, specificity, and accuracy of TIC categorization by the manual method and semi-automatic method are shown in Table 3. The sensitivity was slightly lower, but the semi-automatic method significantly improved the specificity and accuracy ($P = 2.43 \times 10^{-6}$). Thus, the proposed semi-automatic method can help radiologists discriminate breast IDCs and benign lesions using DCE-MRI.

Discussion

Compared with other imaging methods, DCE-MRI has many advantages, for example, it is noninvasive, does not use radiation and has better soft tissue contrast. Not only can DCE-MRI detect lesions that cannot be visualized by mammography or ultrasound [17], but it can also detect multiple lesions in ipsilateral or contralateral breast regions [18, 19]. The American Cancer Society recommends that women with a high risk of breast cancer are candidates for breast MRI screening [20, 21]. However, in China, only symptomatic patients can be referred for MRI examinations due to limited medical resources. DCE-MRI has high sensitivity for breast cancer but its specificity is variable [22, 23]. In addition, the manual method based on an MRI work station leads to intra- and inter-observer variability, partial volume effects, and it is time consuming [24]. To improve the specificity of MRI and address these issues, computer-aided detection has been employed widely to evaluate quantitative parameters in the analysis of breast lesions [24–27]. Chang et al. used the fuzzy c-means clustering technique to extract a representative TIC [28]. Levman measured the tumor's margin to facilitate the diagnosis of breast cancer [29]. In the present study, we semi-automatically extracted lesions from the subtracted images using the OTSU method. The lesion extraction results showed that the mass-like lesions were



determined correctly, and the necrotic areas in IDCs were also excluded from the lesions.

Previous studies have shown that the tumor morphology and TIC washout pattern obtained from breast DCE-MR images are the strongest predictors of breast cancer [30–32]. The different TIC patterns can discriminate malignant and benign lesions. A persistent pattern is associated with a greater likelihood of a benign lesion, and the washout pattern is associated with a higher likelihood of a malignant lesion. The plateau pattern is seen in both malignant and benign lesions, but type II is considered to be suggestive of malignancy. Our TIC quantitative categorization results yielded the same conclusion. According to the SI_{slope} value calculated from the mean curve, 80.4% of the lesions categorized as type I were benign lesions and 81.8% of the lesions categorized as type III were breast IDCs. In the present study, 42 lesions (10 benign lesions and 32 malignant lesions) were categorized as type II according to the SI_{slope} value. Based on the results obtained by the regression model using the mean curve, the diagnostic accuracy was 73.8% (four benign lesions and 27 malignant lesions) for the plateau pattern. Compared with the categorization results produced by the manual method, the proposed method for quantitative lesion categorization exhibited higher diagnostic performance.

The TIC washout pattern is a feature of breast cancer, so previous studies have suggested that the quantitative parameters derived from TIC may be useful for diagnosis. However, previous studies have not considered combining these parameters for breast diagnosis. The results produced

using the regression models demonstrated that ESER, MSI, and SI_{slope} were the meaningful indicators of breast IDCs, while the three other parameters were not significant in predicting malignancy (independent samples t test, $P > 0.05$). Indeed, from Eqs. (1), (2), and (5), we can see that ESER and MSI represent the enhancement of the lesion, whereas SI_{slope} represents the reduction in the signal intensity. The cases with greater ESER and MSI were more likely to indicate breast IDCs, while the cases with greater SI_{slope} were potentially associated with benign lesions. For the lesion region identified from the semi-automatic method, the optimal cutoff value of the regression model larger than 0.1215 was considered significant with respect to malignancy, while for the mean curve, the optimal cutoff value was 0.0644. For the manual method, the optimal cutoff value for MSI was 884.427. As mentioned in previous studies, the TICs of breast IDCs appear to be obviously enhanced with more rapid metabolism due to the large micro-vessel density within the lesions, whereas benign lesions exhibit more gradual inflow and outflow of the contrast agent [33, 34]. Thus, the results obtained by our regression models were consistent with previous findings. Our results showed that the regression model based on the semi-automatically determined lesion regions had the best breast lesion diagnosis performance (AUC 0.846, sensitivity 81.7%, specificity 80.3%, and accuracy 81.0%) and it performed significantly better than the MSI obtained using the manual method. Thus, the regression models could be useful for discriminating IDCs and benign lesions by breast DCE-MRI, potentially reducing the need to biopsy or remove benign lesions.

Table 2 Results of the logistic regressions for the quantitative parameters and the ROC analysis

	Mean curve			Lesion region			Manual method
	ESER	MSI	SI_{slope}	ESER	MSI	SI_{slope}	MSI
β_X	0.516	0.479	-0.521	0.569	0.492	-0.565	/
SE (β_X)	0.115	0.107	0.117	0.124	0.107	0.123	/
U	4.487*	4.477*	-4.453*	4.589*	4.598*	-4.593*	/
OR	1.033	1.001	0.982	1.035	1.001	0.984	/
β	0.0323	0.00136	-0.0184	0.0345	0.00146	-0.0165	/
Logistic model	0.0323 × ESER + 0.00136 × MSI - 0.0184 × SI_{slope} - 3.585			0.0345 × ESER + 0.00146 × MSI - 0.0165 × SI_{slope} - 3.801			/
AUC	0.837			0.846			0.604
SE	0.0427			0.0417			0.0572
95% CI	(0.754, 0.900)			(0.762, 0.912)			(0.503, 0.699)
Optimal cutoff	> 0.0644			> 0.1215			> 884.427
Sensitivity	80.3%			81.7%			64.7%
Specificity	77.4%			80.3%			62.0%
Accuracy	78.9%			81.0%			63.35%

CI confidence interval, SE standard error, β_X estimate of standardized parameters, β estimate of original parameters, OR odds ratio

*Significant difference

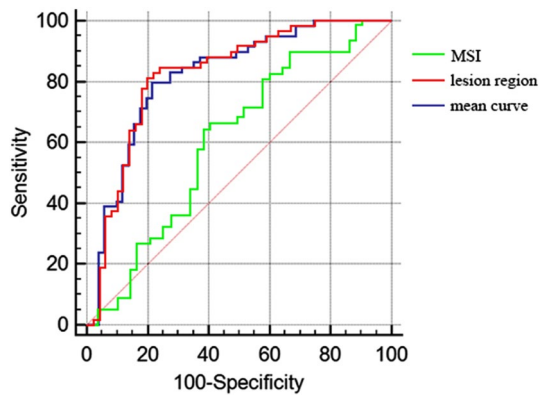


Fig. 5 Results of the ROC curve analysis

Table 3 Comparison of the TIC categorization results obtained by the conventional manual method and the new semi-automatic method

	Manual method (%)	Semi-automatic method (%)
Sensitivity	85.92	81.69
Specificity	32.39	70.42
Accuracy	59.16	76.05

This study had several limitations. First, the number of patients included was relatively small. Second, because only solitary mass-like lesions were included and the malignant cases were only IDCs, the tumor types and their proportions might influence the results. Third, only TIC from breast DCE-MRI was analyzed semi-automatically, and lesion morphology was not considered as an analysis target. In fact, some previous studies have suggested that the TIC pattern should be analyzed after evaluating the morphology of lesions [26, 27]. We believe the diagnostic performance would be improved if the morphology of lesions and the parameters derived from the TICs were combined. Hence, further research should be carried out. Fourth, breast MRI analyses have been conducted with volume images, but our study used two-dimensional images.

Regardless of these limitations, our study is the first to investigate a semi-automatic method for distinguishing breast IDCs and benign lesions using regression models based on multiple parameters derived from the TICs by DCE-MRI. The proposed method has high sensitivity and specificity in the diagnosis of breast IDCs.

Acknowledgements This work was supported by Startup Foundation for Doctors of Liaoning Province (no. 201601118).

Compliance with ethical standards

Conflict of interest The authors declare that they have no conflict of interest.

References

- Jemal A, Bray F, Center MM et al (2011) Global cancer statistics. *CA Cancer J Clin* 61(2):69–90
- Mayrhofer RM, Ng HP, Putti TC et al (2013) Magnetic resonance in the detection of breast cancers of different histological types. *Magn Reson Insights* 6(6):33–49
- Weinstein SP, Localio AR, Conant EF et al (2009) Multimodality screening of high-risk women: a prospective cohort study. *J Clin Oncol* 27(36):6124–6128
- Lehman CD, Isaacs C, Schnall MD et al (2007) Cancer yield of mammography, MR, and US in high-risk women: prospective multi-institution breast cancer screening study. *Radiology* 244(2):381–388
- Kumar A, Srivastava V, Singh S et al (2010) Color Doppler ultrasonography for treatment response prediction and evaluation in breast cancer. *Future Oncol* 6(8):1265–1278
- Karellas A, Vedantham S (2008) Breast cancer imaging: a perspective for the next decade. *Med Phys* 35(11):4878–4897
- Brennan M, Spillane A, Houssami N (2009) The role of breast MRI in clinical practice. *Aust Fam Physician* 38(7):513–519
- Kuhl CK (2007) Breast MR imaging at 3T. *Magn Reson Imaging Clin N Am* 15(3):315–320
- Kim JY, Kim SH, Kim YJ et al (2015) Enhancement parameters on dynamic contrast enhanced breast MRI: do they correlate with prognostic factors and subtypes of breast cancers? *Magn Reson Imaging* 33(1):72–80
- Li X, Arlinghaus LR, Ayers GD et al (2014) DCE-MRI analysis methods for predicting the response of breast cancer to neoadjuvant chemotherapy: pilot study findings. *Magn Reson Med* 71(4):1592–1602
- Jansen SA, Lin VC, Giger ML et al (2011) Normal parenchymal enhancement patterns in women undergoing MR screening of the breast. *Eur Radiol* 21(7):1374–1382
- Abramson RG, Li X, Hoyt TL et al (2013) Early assessment of breast cancer response to neoadjuvant chemotherapy by semi-quantitative analysis of high-temporal resolution DCE-MRI: preliminary results. *Magn Reson Imaging* 31(9):1457–1464
- Platel B, Mus R, Welte T et al (2014) Automated characterization of breast lesions imaged with an ultrafast DCE-MR protocol. *IEEE Trans Med Imaging* 33(2):225–232
- Otsu N (1979) A threshold selection method from gray-level histograms. *IEEE T Syst Man CY S* 9(1):62–66
- Kuhl CK, Mielcareck P, Klaschik S et al (1999) Dynamic breast MR imaging: are signal intensity time course data useful for differential diagnosis of enhancing lesions? *Radiology* 211(1):101–110
- Montemurro F, Martincich L, Sarotto I et al (2007) Relationship between DCE-MRI morphological and functional features and histopathological characteristics of breast cancer. *Eur Radiol* 17(6):1490–1497
- Tozaki M (2013) BI-RADS-MRI terminology and evaluation of intraductal carcinoma and ductal carcinoma in situ. *Breast Cancer* 20(1):13–20
- Morris EA (2010) Diagnostic breast MR imaging: current status and future directions. *Magn Reson Imaging Clin N Am* 18(1):57–74
- Lehman CD, Gatsonis C, Kuhl CK et al (2007) MRI evaluation of the contralateral breast in women with recently diagnosed breast cancer. *N Engl J Med* 356(13):1295–1303
- Saslow D, Boetes C, Burke W et al (2007) American Cancer Society guidelines for breast screening with MRI as an adjunct to mammography. *CA Cancer J Clin* 57(2):75–89
- Sardanelli F, Boetes C, Borisch B et al (2010) Magnetic resonance imaging of the breast: recommendations from the EUSOMA working group. *Eur J Cancer* 46(8):1296–1316

22. Yabuuchi H, Matsuo Y, Okafuji T et al (2008) Enhanced mass on contrast-enhanced breast MR imaging: Lesion characterization using combination of dynamic contrast-enhanced and diffusion-weighted MR images. *J Magn Reson Imaging* 28(5):1157–1165
23. Pinker-Domenig K, Bogner W, Gruber S et al (2012) High resolution MRI of the breast at 3 T: which BI-RADS(A) descriptors are most strongly associated with the diagnosis of breast cancer? *Eur Radiol* 22(2):322–330
24. Renz DM, Böttcher J, Diekmann F et al (2012) Detection and classification of contrast-enhancing masses by a fully automatic computer-assisted diagnosis system for breast MRI. *J Magn Reson Imaging* 35(5):1077–1088
25. Levman JE, Causer P, Warner E et al (2009) Effect of the enhancement threshold on the computer-aided detection of breast cancer using MRI. *Acad Radiol* 16(9):1064–1069
26. Retter F, Plant C, Burgeth B et al (2013) Computer-aided diagnosis for diagnostically challenging breast lesions in DCE-MRI based on image registration and integration of morphologic and dynamic characteristic. *EURASIP J Adv Signal Process.* 2013:157. <https://doi.org/10.1186/1687-6180-2013-157>
27. Agliozzo S, De Luca M, Bracco C et al (2012) Computer-aided diagnosis for dynamic contrast-enhanced breast MRI of mass-like lesions using a multiparametric model combining a selection of morphological, kinetic, and spatiotemporal features. *Med Phys* 39(4):1704–1715
28. Chang YC, Huang YH, Huang CS et al (2012) Classification of breast mass lesions using model-based analysis of the characteristic kinetic curve derived from fuzzy c-means clustering. *Magn Reson Imaging* 30(3):312–322
29. Levman JE, Martel AL (2011) A margin sharpness measurement for the diagnosis of breast cancer from magnetic resonance imaging examinations. *Acad Radiol* 18(12):1577–1581
30. Baum F, Fischer U, Vosschenrich R et al (2002) Classification of hypervascularized lesions in CE MR imaging of the breast. *Eur Radiol* 12(5):1087–1092
31. Kinkel K, Helbich TH, Esserman LJ et al (2000) Dynamic high-spatial-resolution MR imaging of suspicious breast lesions: diagnostic criteria and interobserver variability. *AJR Am J Roentgenol* 175(1):35–43
32. El Khouli RH, Macura KJ, Jacobs MA et al (2009) Dynamic contrast-enhanced MRI of the breast: quantitative method for kinetic curve type assessment. *AJR Am J Roentgenol* 193(4):295–300
33. Hayes C, Padhani AR, Leach MO (2002) Assessing changes in tumor vascular function using dynamic contrast-enhanced magnetic resonance imaging. *NMR in Biomedicine* 15(2):154–163
34. Hauth EA, Jaeger H, Maderwald S et al (2006) Evaluation of quantitative parametric analysis for characterization of breast lesions in contrast-enhanced MR mammography. *Eur Radiol* 16(12):2834–2841

Publisher's Note Springer Nature remains neutral with regard to jurisdictional claims in published maps and institutional affiliations.